Appication of Fracture Mechanics to Paper Strength

종이의 강도적 특성에 대한 파괴역학적 해석

Jong-Moon Park[1] and James L. Thorpe[2]

[1] School of Forest Resources, Chungbuk Nat'l Univ., Cheongju 361-763, Korea.

[2] College of Environmental Science & Forestry, State Univ. of New York, Syracuse, NY 13210, USA.

1. Introduction

Paper is not a perfect material. Paper contains a lot of voids and imperfection. We may think a paper as a structure of cracks in it. When an external load is applied to a paper, cracks will grow. We may consider a structure in which a crack develops. Due to the application of repeated loads or due to a combination of loads and environmental attack this crack will grow with time. The crack propagation as a function of time can be represented by a rising curve. Due to the presence of the crack the strength of the structure is decreased. The residual strength of the structure decreases progressively with increasing crack size. According to a traditional textbook, Fracture mechanics is able to answer the following questions. "a. The residual strength as a function of crack size, b. What size of crack can be tolerated at the expected service load; i.e. what is the critical crack size? c. How long does it take for a crack to grow from a certain initial size to the critical size? d. What size of pre-existing flaw can be permitted at the moment the structure starts its service life? e. How often should the structure be inspected for cracks?"

When the stress at a crack tip is thought, a crack in a solid can be stressed in 3 different modes, as Mode I, II, and III. Mode I is an opening mode, Mode II is sliding mode, and Mode III is tearing mode. Usually paper is under opening mode situation. The elastic stress field in mode I loading can be calculated. In the coordinate system of distance and angle (r, θ), the in-plane crack tip stresses always can be expressed as

$$\sigma_{ij} = K_I/(\sqrt{2\pi r}) \; f_{ij}(\theta)$$

The functions $f(\theta)$ are already known functions of θ. Since K_I describes all the crack tip stresses it is an important parameter, called the stress intensity factor. The crack tip stresses can now be written as

$$\sigma_x = \sigma \sqrt{\frac{a}{2r}} \cos\frac{\theta}{2}[1 - \sin\frac{\theta}{2} \sin\frac{3\theta}{2}]$$

$$\sigma_y = \sigma \sqrt{\frac{a}{2r}} \cos\frac{\theta}{2}[1 + \sin\frac{\theta}{2} \sin\frac{3\theta}{2}]$$

$$\tau_{xy} = \sigma \sqrt{\frac{a}{2r}} \sin\frac{\theta}{2} \times \cos\frac{\theta}{2} \times \cos\frac{3\theta}{2}]$$

Above equations provide the stresses for an area close to the crack tip only. For large r(at remote area) all the stresses tend to zero, which cannot be correct. Indeed, the complete stress field is given by

$$\sigma_{ij} = K_I/(\sqrt{2\pi r}) + \text{2nd term} + \text{3rd term} + \text{4term} + \ldots$$

First equation is an elastic solution, the stresses become infinite at the crack tip, in reality this cannot occur: plastic deformation taking place at the crack tip keeps the stresses finite. An impression of the size of the crack tip plastic zone can be obtained. Total length of plastic deformation r_p* can be calculated by the following equation.

$$\sigma_{ij} = K_I/(\sqrt{2\pi\ r_p{}^*}) = \sigma_{ys} \text{ (yield stress)}$$
$$\therefore r_p* = K_I{}^2 / \{ 2\ \pi(\sigma_{ys})^2 \} = \sigma^2 a / \{ 2\ (\sigma_{ys})^2 \}$$

r_p* can be directly expressed as a function of the stress intensity factor and the yield stress. Generally, above equation will apply only as long as the plastic zone is so small. Stress intensity factor K_I is a known function of crack size and sample's width (shape factor).

J-integral provides a means to determine an energy release rate for cases where plasticity effects are not negligible. There several ways to measure J-integral. One of simple methods is as follows;

$$J = 2 A / \{ B \times (W - a) \}$$

Where A is an area of load-elongation curve, B is sample's thickness, W is sample's total width, and a is crack length.

Principal factors controlling press room breaks have been studied by Uesaka recently. Press room runnability problems, such as web break is very important issue. Recent trends in press rooms are increased emphasis on productivity, increased press speed, and

increased use of multi colours. Those trends ask to upgrade paper performance more than ever. In spite of the overwhelming amount of information generated from studies, there is, surprisingly, no data showing a clear quantitative relationship between press room breaks and many variables. One of the reasons for the lack of quantitative data is that breaks are very rare phenomena. Another reason is that there are always multiple random variables involved in the phenomena. In order to understand the interactions between paper(or mill) variables and press room variables, web strength variations, defect distributions, and tension applied in the press unit can be considered. These are important factors of fracture mechanics.

Lets think about tensile energy absorption and strain energy density of paper. Strain fields at the tip of a crack define the yield process in paper under tensile loading. A series of strain fields at increasing load intervals details the rate of crack propagation. Interestingly, when the crack propagates it is not as a single line, but as a three dimensional strain volume. The strain volume grows as the crack propagates causing new material to be deformed. As the deformation area increases in size an ever increasing amount of energy is put into the paper to maintain the necessary strain concentration for the expanding volume of crack growth. This ever increasing deformation becomes the source of energy absorption within the sheet and stable crack growth.

Can the energy required for stable crack growth be quantified? If it is quantified, will it measure a useful physical property of that particular grade of paper? The answer to both of these questions is yes. By combining local stresses with local strains and summing the resultant quantities over the area of interest yields the aggregate of energy or internal work of that particular paper. The conventional phrase to describe this quantity is strain energy density. But, where do the stress values come from? There is no experimental method to define stress over multiple local areas within a paper sample. The answer is from finite element analysis (FEA) simulation. The stress field within tensile specimens in mode I fracture can be simulated giving a good estimate of local stresses. Kraft sack is contrasted with newsprint to show the differences in the strain profiles, the stress profiles and the strain energy density profiles in mode I tensile loading.

1. 1 Theory

The stress on each volume element of paper is not always the same. Therefore, the

total strain energy in the entire structure is obtained by taking the integral over the volume of paper:

Strain energy U(P) at a certain load level, P, is given by

$$U(P) = \int_V D \; dV \qquad\qquad [1]$$

Where V is a volume of a whole sheet. The strain energy density, D, is obtained from the integration of stress with elastic plus plastic strain over the complete loading history, and in each load increment i the contribution at point j is

$$\triangle U_j = \triangle D_j \times \triangle V_j$$

$$\text{Where } \triangle D_j = (\sigma_i + \frac{1}{2}\triangle \sigma_i)(\triangle \varepsilon_i^{\,e} + \triangle \varepsilon_i^{\,p}) \qquad\qquad [2]$$

Where superscripts 'e' and 'p' denote elastic and plastic components respectively, and $\triangle V_j$ is the volume associated with point j such that $\sum \triangle V_j$ = V. Therefore, integration over the whole structure and for all load increments up to load, P, gives

$$U(P) = \sum_i \sum_j (\sigma_i + \frac{1}{2}\varDelta \sigma_i)(\varDelta \varepsilon_i^{\,e} + \varDelta \varepsilon_i^{\,p}) \; \varDelta V_j \qquad\qquad [3]$$

The stresses and strains, for stationary cracks, around crack tip of elastic-plastic material has been derived theoretically under yielding conditions [13]. The strains and stresses can be obtained from the following equations at varying yielding conditions from small-scale to fully plastic. From the strain and stress equations, the strain energy density equation is derived from the following equations.

$$\varepsilon_{ij} = \varepsilon_0 \left(\frac{EJ}{\sigma_o^{\,2}} I_n \, r \right)^{-\frac{n}{n+1}} \bar{\varepsilon}_{ij}(\theta, \, n) \qquad\qquad [4]$$

$$\sigma_{ij} = \sigma_0 \left(\frac{EJ}{\sigma_o^{\,2}} I_n \, r \right)^{-\frac{1}{n+1}} \bar{\sigma}_{ij}(\theta, \, n) \qquad\qquad [5]$$

$$D = \frac{n}{n+1} \frac{\pi}{I_n} \frac{\sigma^{\,2}}{r} \bar{\sigma}_e^{\,n+1} \qquad\qquad [6]$$

Where, E is an elastic modulus of the sheet with cracks defined as yield stress/yield strain, σ_0 / ε_0; J is J-integral, which is defined by the path independent line integral [4, 5]; r and θ are polar coordinates of crack tip, namely distance and angle respectively; I_n is a numerical constant which is a function of n, the straining hardening exponent; $\bar{\varepsilon}_{ij}(\theta,n)$, $\bar{\sigma}_{ij}(\theta,n)$, and $\bar{\sigma}e$ are known dimensionless functions of the circumferential position θ and n; σ is remote stress at loading point; and D is strain energy density.

Under tensile load, a material with cracks experiences high stresses around the cracks. Many materials including paper usually exhibit some plastic deformation prior to fracture. Depending on the extent of plasticity, different fracture mechanics theory should be applied because of the assumptions involved. Therefore, depending on the extent of plasticity, it is useful to distinguish four regimes of yielding as shown in Fig. [6]. The local stress near the crack tip is expressed as σ_l, uniaxial yield stress as σ_y, net section stress as σ_n which is the stress at the ligament, and the uniform remote stress from the crack is expressed as σ. Fig. 1. a shows the small scale yield case ($\sigma_l > \sigma_y > \sigma_n > \sigma$) which has a yield zone vanishingly small in the immediate vicinity of the crack. In the contained yield case ($\sigma_l > \sigma_y \geq \sigma_n > \sigma$) as shown in Fig. 1. b, the yielding zone is contained within the structure but does not spread to a lateral boundary of the structure. Fig. 1. c is the gross yield case ($\sigma_l > \sigma_n \geq \sigma_y > \sigma$) which has a very extensive yielding zone spreading to the lateral boundary ahead of the crack and is, thus, not contained. In the general yield case ($\sigma_l > \sigma_n > \sigma > \sigma_y$) as shown in Fig. 1. d, extensive plasticity spreads across the whole area because the applied stress, σ, is greater than the yield stress, σ_y.
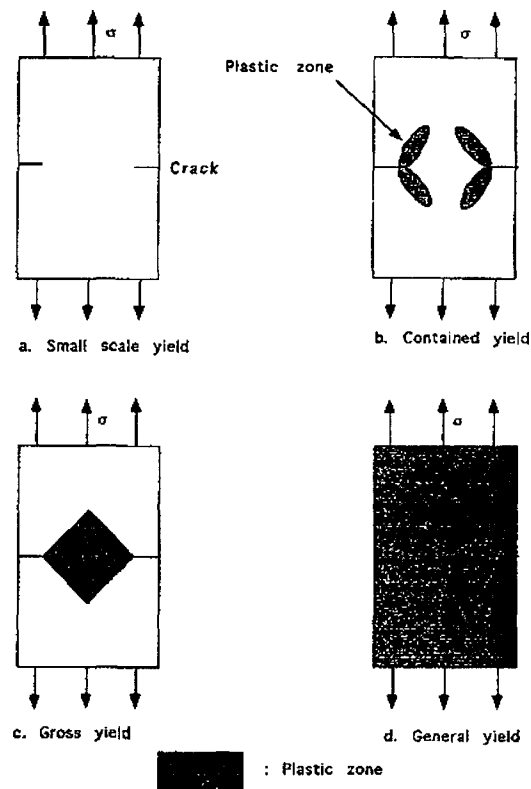

Fig. 1. Schematic representation of four regimes of yield.

Linear elastic fracture mechanics (LEFM) may be applied to small scale yield and contained yield. Elastic-plastic fracture mechanics (EPFM) may be applied to contained yield, gross yield and general yield. Recently post-yield fracture mechanics (PYFM) has been proposed for gross yield and general yield[6]. As a fracture criterion, different parameters are used for different yield as summarized in Table 1. They are stress intensity factor , K_c , J-integral, J_c , and strain energy density, D_c, where subscript c means critical value. Gross yield and general yield can be observed in tough paper on tensile loading, where strain energy density can be used as a fracture criterion. Therefore, in this study, strain energy density is observed and analyzed.

1. 1. 1 Strain energy density

Analysis of strain energy density of small localized areas is important to understand the fracture phenomena of paper, because paper is a non-homogeneous non-isotropic material. Strain energy density has been reported as a failure criterion for a material with flaws[7, 8]. According to the criterion, failure initiates when the strain energy stored in a unit volume of material ahead of the notch reaches a critical value. This value corresponds to the area under the stress/strain curve.

There are two sources of energy that can be supplied to extend the crack. One is from the work done by the applied external load and the other is the strain energy stored in the structure during deformation by the applied external load. the latter type of energy increases with crack propagation, as the structure's capacity to store the strain energy decreases. The compliance, which is defined as the deformation per unit load, increases as the crack propagates[9]. As the compliance increases, local structure reaches a limit that the structure can store the strain energy which is defined as strain energy density.

Table 1. Yield classification and its related theory and criterion

Yield classification	Theory	Fracture criterion
a. Small scale yield	LEFM	K_c
b. Contained yield	LEFM, EPFM, PYFM	K_c, J_c, D_c
c. Gross yield	LEFM, EPFM, PYFM	K_c, J_c, D_c
d. General yield	EPFM, PYFM	J_c, D_c

2. Materials and Methods

Double-edge notched specimens were used as described in previous work[10]. The image observation area was 280 pixels by 400 pixels. That area was broken into 280 strain observation elements, a 14 by 20 grid of elements, each 2.61 mm wide by 2.12 mm high. The total size of observation area is 365 mm width and 423 mm height. The finite element analysis grid for calculating stresses was identical in size.

In this study, stresses were obtained from isoparametric quadrilateral 8 node elements in three dimensions with ANSYS Engineering Finite Element Analysis System[11]. Specimen is symmetric to horizontal and vertical axies, so one-quarter of specimen is analyzed by 207 nodes and 182 elements as shown in Fig. 2. Near the crack tip, more refined elements are produced and the crack tip solid element is used to incorporate the inverse square root singularity of displacement field.
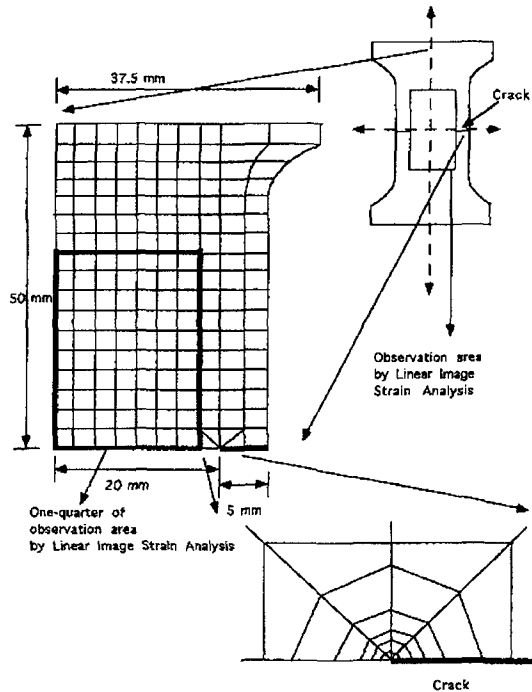

Fig. 2. Nodes and elements for finite element analysis.

3. Results and Discussion

3. 1 Results
3. 1. 1 Strain profiles

The strain profiles at increasing load increments in the cross machine direction of the kraft sack are shown in Fig. 3. The cross-machine direction strain profiles of newsprint at increasing load increments are shown in Fig. 4. The kraft sack cross-machine direction strain profiles are shown in Fig. 3. a - 3. c. The total strain to failure was 2.72% at a load of 20.8 kgf. In Fig. 3. a at a whole specimen strain of 1.08% the strain region above 2.5% emerges. In Fig. 3. b, at a whole specimen strain of 1.73%, a region of strain above 3.0% appears not only at the crack tip, but also in isolated upper
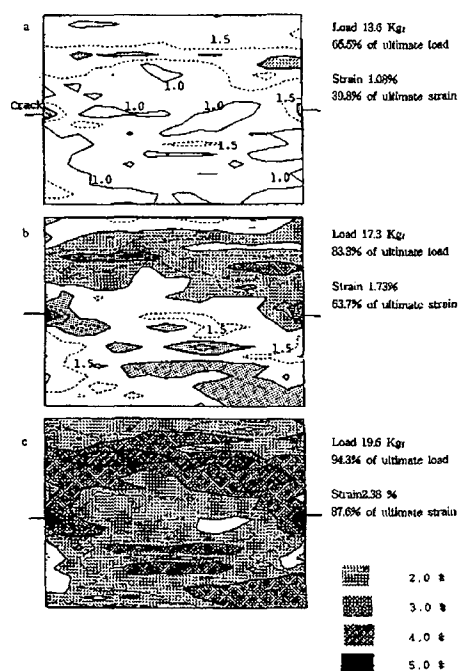
Load 13.6 Kg,
65.5% of ultimate load

Strain 1.06%
39.8% of ultimate strain

Load 17.3 Kg,
83.3% of ultimate load

Strain 1.73%
63.7% of ultimate strain

Load 19.6 Kg,
94.3% of ultimate load

Strain 2.38 %
87.6% of ultimate strain

2.0 %
3.0 %
4.0 %
5.0 %

Fig. 3. Strain(unit: %) profiles of kraft sack paper in the cross-machine direction.

Load 2.7 Kg,
70.0% of ultimate load

Strain 0.87%
65.7% of ultimate strain

Load 3.1 Kg,
81.4% of ultimate load

Strain 1.08%
82.1% of ultimate strain

Load 3.5 Kg,
91.4% of ultimate load
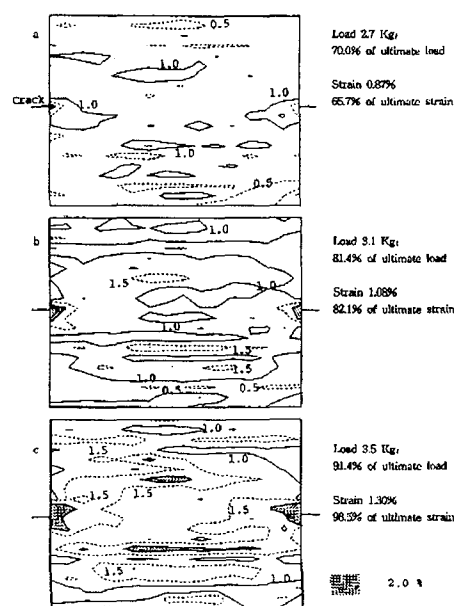
Strain 1.30%
98.5% of ultimate strain

2.0 %

Fig. 4. Strain(unit:%) profiles of newsprint in the cross-machine direction.

locations. The length of isolated regions with 3% strain reaches 15 mm at the distance of 15 mm from the crack tip. The area covered by strains greater than 3.0% is now approximately 330 mm². In Fig. 3. c, at a whole specimen strain of 2.38%, the strain region above 3.0% has widened and is connected to the upper location.

The strain profiles of the newsprint cross-machine direction are shown in Figs. 4. a - 4. c. The total strain to failure was 1.32% at a load of 3.83 kgf. Fig. 4. a is a strain profile at a whole specimen strain of 0.87% The region of above 2% has been observed in front of the crack tip. In Fig. 4. b, at a whole specimen strain of 1.08%, strains above 3.0% appear at the crack tip. Isolated areas above 1.5% strain have a total strain area of 40 mm². In Fig. 4. c, at a whole specimen strain of 1.30%, the area of the strain region above 1.75% approaches 200 mm².

3. 1. 2 Stress distribution

The kraft sack stress profiles of cross-machine direction are shown in Fig. 5. a - 5. c. In Fig. 5. a, the regions above 1.75 Kg$_f$/mm² stress are shown in front of the crack tip at
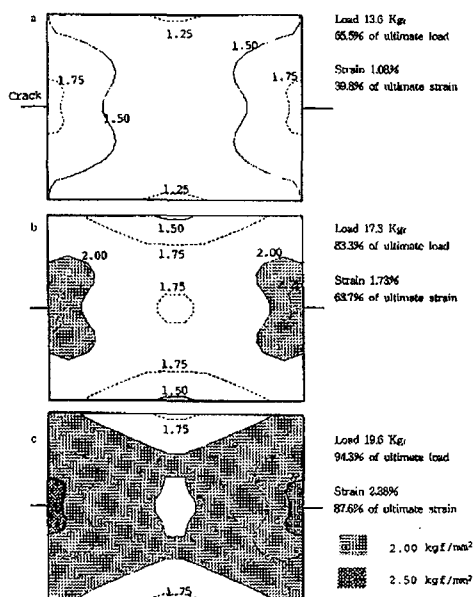
Fig. 5. Stress(unit:kgf/m^2) profiles of kraft sack paper in the cross-machine direction(failure load = 20.8 kgf, failure strain = 2.72%).
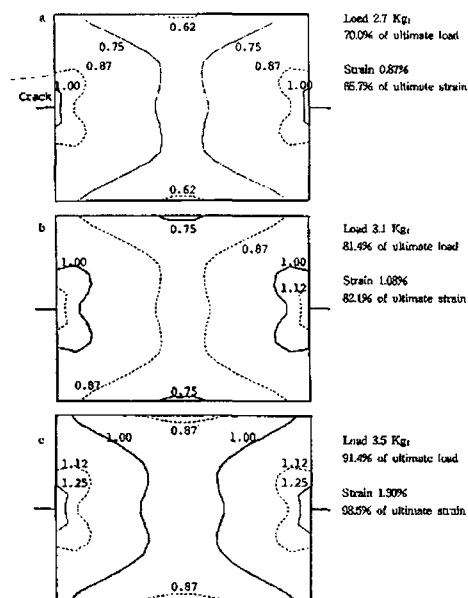
Fig. 6. Stress(unit:kgf/m^2) profiles of newsprint in the cross-machine direction(failure load 3.8 kgf, failure strain = 1.32%).

13.6 Kg$_f$ load. In Fig. 5. b, the regions of 2.25 Kg$_f$/mm^2 stress start to appear at 17.3 Kg$_f$ load. In Fig. 5. c at 19.6 Kg$_f$ load, the regions above 2.50 Kg$_f$/mm^2 stress is shown in front of the crack tip. At the center location, the region below 2.00 Kg$_f$/mm^2 stress appears.

The newsprint stress profiles of cross-machine direction are shown in Fig. 6. a - 6. c. In Fig. 6. a, the regions above 1.00 Kg$_f$/mm^2 stress are shown in front of the crack tip at 2.7 Kg$_f$ load. In Fig. 6. b, the regions of 1.125 Kg$_f$/mm^2 stress start to appear at 3.1 kgf load. In Fig. 6. c at 3.5 Kg$_f$ load, the regions above 1.25 Kg$_f$/mm^2 stress are shown in front of the crack tip.

3. 1. 3 Strain energy density

The strain energy density profiles of kraft sack and newsprint are shown in Figs. 7. a - 7. c and 8. a - 8. c, respectively. The strain energy density has units of Kg$_f$/mm^2. In Fig. 7. a, at 13.6 Kg$_f$ load, the strain energy density of 2.50 ×10^{-2} Kg$_f$/mm^2 starts to appear in front of the crack tip. The strain energy density of 1.00 ×10^{-2} Kg$_f$/mm^2 is extended 38 mm from the crack tip. In Fig. 7. b, at 17.3 kgf load, the strain energy
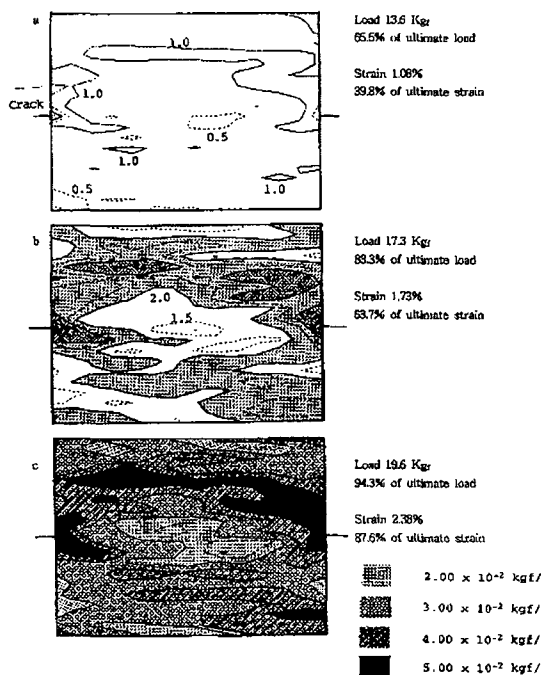
Load 13.6 Kgf
65.5% of ultimate load

Strain 1.08%
39.8% of ultimate strain

Load 17.3 Kgf
83.3% of ultimate load

Strain 1.73%
63.7% of ultimate strain

Load 19.6 Kgf
94.3% of ultimate load

Strain 2.38%
87.5% of ultimate strain

2.00 x 10⁻² kgf/
3.00 x 10⁻² kgf/
4.00 x 10⁻² kgf/
5.00 x 10⁻² kgf/

Load 2.7 Kgf
70.0% of ultimate load

Strain 0.87%
65.7% of ultimate strain

Load 3.1 Kgf
81.4% of ultimate load

Strain 1.08%
82.1% of ultimate strain

Load 3.5 Kgf
91.4% of ultimate load

Strain 1.30%
98.5% of ultimate strain

1.00 x 10⁻² kgf/m
1.50 x 10⁻² kgf/m
2.00 x 10⁻² kgf/m

Fig. 7. Strain energy(unit:x10⁻² kgf/m²) profiles of
kraft sack paper in the cross-machine direction
(failure load = 20.8 kgf, failure strain = 2.72%).
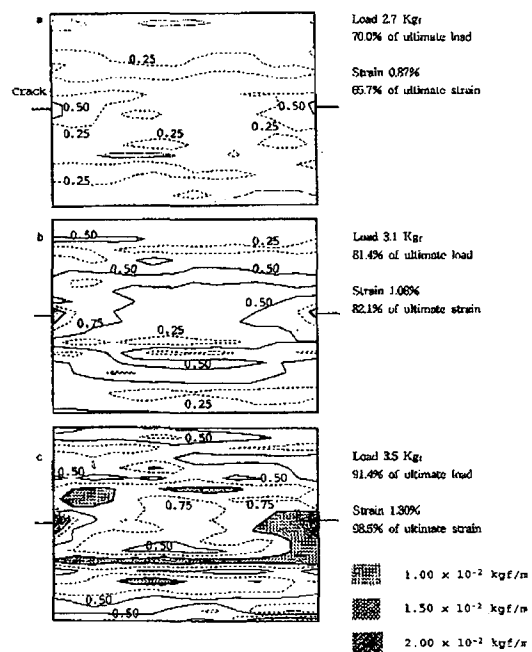
Fig. 8. Strain energy density(unit:x10⁻² kgf/m²) profiles
of newsprint in the cross-machine direction
(failure load = 3.8 kgf, failure strain = 1.32%).

density of 5.00 $\times 10^{-2}$ Kgf/mm² is observed at the crack tip. Even with this high strain energy density value, whole specimen sustains its external loading without fracture. Areas of the strain energy density of $2.50-3.00 \times 10^{-2}$ Kgf/mm² are connected. The total area of the strain energy density above 2.00×10^{-2} Kgf/mm² is about 900 mm². In Fig. 7. c, at 19.6 Kgf load, most of the observation area has the strain energy density greater than 3.00×10^{-2} Kgf/mm².

In Fig. 8. a, at 2.7 Kgf load, the strain energy density becomes slightly greater than 0.5 $\times 10^{-2}$ Kgf/mm². In Fig. 8. b, at 3.1 Kgf load, high strain energy density above 1.00 $\times$ 10^{-2} Kgf/mm² is apparent at the crack tip. Most of the observation area has a strain energy density value of 0.25 $\times 10^{-2}$ Kgf/mm². The area of the strain energy density above 0.50 Kgf/mm² is about 500 mm². In Fig. 8c, at 3.5 Kgf load, strain energy density above 2.50 $\times 10^{-2}$ Kgf/mm² is observed at the crack tip. Areas of 1.00 $\times 10^{-2}$ Kgf/mm² strain energy density are connected crack tip to crack tip.

The strain energy density of each element is summed throughout the whole

observation area. The strain energy values of kraft sack paper are 2.45, 6.52, and 11.78 $Kg_f \cdot mm$ for whole observation area of Fig. 7. a, 7. b, and 7. c, respectively. The strain energy values of newsprint are 0.20, 0.49, and 0.81 $Kg_f \cdot mm$ for the whole observation area of Fig. 8. a, 8. b, and 8. c, respectively.

3. 2 Discussion

3. 2. 1 Strain profiles

There are apparent differences between kraft sack paper and newsprint in strain profile development. These two grades contrast the differences between the strain profiles of a tough paper and a weak paper. Kraft sack paper in the cross-machine direction has widely distributed areas of sub-critical strain before the ultimate failure of the sample. When the critical tensile load is reached, some of the highly strained areas are connected and the sample fails. The shape of sub-critical strain area is two-directional with a barrier at the center of the crack tip. By contrast, the newsprint cross-machine direction has narrower distributed areas of sub-critical strain just before the ultimate failure of the sample than the kraft sack paper. Even when the critical tensile load is approached, highly strained areas are not connected as is shown in Fig. 4. c, but concentrated around the crack tip.

3. 2. 2 Strain energy density

Strain energy density is calculated from the summation of individual element strains and the stresses with equation [3]. Strain energy density is usually high near the crack tip, because the strains and stresses are high near the crack tip. The stress becomes stable and approaches to the average stress value of whole specimen at 5 mm from the crack tip.

The strain energy density of kraft sack before failure in front of the crack tip covers a wide area over 5.00×10^2 Kg_f/mm^2. By contrast, newsprint has a small area which has strain energy density of 2.50×10^2 Kg_f/mm^2 in front of the crack tip. The wide area of high strain energy density for kraft sack paper can be related to the blunting phenomenon in front of the crack tip. Blunting is due to plastic deformation[4]. When sufficient plastic deformation can occur to relieve stresses, fracture will be postponed. Blunting is a relaxation process that distributes stress concentration. Local blunting in front of the crack tip ameliorate conditions through lower stresses and larger plastic

strains to absorb the applied energy by the external load. Thus, kraft sack has a wide area of high strain energy density and fracture is delayed by having extensive blunting. The extent of stress concentration is determined by the shape of crack tip during the fracture process whether it is sharp or blunted. If the crack tip is sharp, the extent of stress concentration increases and stable crack growth will be rapid. Therefore, the magnitude of blunting is closely related to the toughness of material. When a material has significant blunting, it gives the higher toughness. This delayed initiation of stable crack growth will result in high strain energy density and additional loading.

When the strain and strain energy density profiles of kraft sack and newsprint are compared, toughness factors can be speculated on. Toughness is determined by the extent of stress and strain during loading. Kraft sack has a high toughness because it has widely distributed high strain profiles that result in a high strain energy density profile before failure. At the same 1.08% strain of whole specimen as shown if Fig. 3. b and 4. c, kraft sack supports 75% more load compared to newsprint when the load is normalized by the basis weight. High toughness than newsprint is given by the better efficiency of kraft sack to support higher load and have widely distributed high strain regions.

The possible reasons for higher toughness of kraft sack can be ascribed to (a) structural effects, like thickness and density of paper, (b) intrinsic fiber strength, (c) fiber bonding, and (d) fiber length. The effects of thickness and density of paper are well known as they increase ; load, which can be supported is increased. The effects of intrinsic fiber strength, fiber bonding, and fiber length on the supportable load will need to be further examined. The plastic region in the stress-strain curve of paper has been ascribed to the rupture of fiber-to-fiber bonds[12]. If this is the case, the widely distributed plastic zones and resulting extensive blunting shown in Fig. 3. c for kraft sack may be related to fiber length, fiber strength, and strong fiber-to-fiber bonding.

The extent of blunting is proportionally related to the magnitude of yield stress and the extent of crack propagation[13]. Yield stress corresponds to the intrinsic fiber strength and fiber length.

Generally, kraft sack paper can be characterized as having long fibers, high fiber bonding, and high intrinsic fiber strength. Whereas, newsprint has short fibers, low fiber bonding, and low intrinsic fiber strength. Therefore, long fiber, high fiber bonding, and high intrinsic fiber strength of kraft sack may be beneficial to high toughness. In kraft sack paper, widely distributed high strain areas show that plastic deformation has

occurred extensively. The plastic deformation causes blunting, thus, fracture is delayed and applied energy is efficiently absorbed. The blunting is a process of sharing applied energy with surrounding area and relaxing stresses which induce high toughness. Further study of the effects of intrinsic fiber strength, fiber bonding, fiber length, and other factors on the paper toughness will show the importance of each factor.

Comparing the strain profiles of kraft sack and newsprint at 1.08% strain, reveals no large dissimilarities. Both show a distribution of 1.5% strains across the ligament between the two crack tips. Both show about the same 2.0% strain area. Both the kraft sack and newsprint began to yield at about 0.5% strain. For some reason, kraft sack is able to strain an additional 1.64% prior to failure while the newsprint strains only an additional 0.24% before failure.

At 1.08% strain kraft sack has 13% of the observation area over 1.5% strain and 2% of the observation area over 2.0% strain. Newsprint at 1.08% strain has 7% of the observation area over 1.5% strain and 0.5% of the observation area over 2.0% strain. Newsprint at 1.30% strain, which is 98.5% of failure strain, has 32% of the observation area above 1.5% strain and 4% above 2% strain.

The mechanism for strain distribution that appears to be similar for both materials reaches a limit for newsprint. The blunting and plastic failures within the newsprint no longer distribute the strains beyond 1.32% strain. The kraft sack is interesting to follow at increasing strain values. At 1.73% strain, 55% of the observation area is below 2.0% strain. Forty-one percent of the observation area is between 2.0% and 3.0% strain, while 4% of the observation area is beyond 3.0% strain. Very little material would appear to have failed completely at this level of strain. At 2.38% strain, 64% of the observation area is below 3.0% strain. Thirty-one percent of the observation area is between 3.0 and 4.0% strain and 5% of the observation area is above 4% strain.

4. Conclusions

Strain energy density can be calculated by combining and summing linear image strain analysis (LISA), local strain values and finite element analysis (FEA), and local stress values, which can be used as a measure of energy absorption within the sheet of paper. The intensity of the stress profile in Mode I fracture depends on the distance and angle from the crack tip. The intensity diminishes with distance from the crack tip. The strain energy density of kraft sack is greater than that of newsprint before failure.

High toughness of kraft sack compared to newsprint can be characterize by widely distributed high strain regions and high strain energy density regions. By having extensive blunting in kraft sack, applied energy is absorbed efficiently and fracture failure is delayed. Possible reasons for high toughness may be related to the intrinsic fiber strength, fiber bonding, fiber length, but more study is required to confirm these factors.

Literature Cited

1. Hutchinson, J. W., J. Mechanics & Physics of Solids, 16(1), 13-31 (1968).
2. Hutchinson, J. W., J. Mechanics & Physics of Solids, 16(4), 337-347 (1968).
3. Rice, J. R., Rosengren, G. F., J. Mechanics and Physics of Solids, 16(1), 1-12 (1968).
4. Rice, J. R., J. Applied Mechanics, 35, 379-386 (1968).
5. Rice, J. R., Mathematical analysis in the mechanics of fracture: Fracture, Liebowitz (ed.). Vol.II, Academic press, New York, NY, p.191-311, 1968.
6. Tuner, C. E., Methods for post-yield fracture safety assessment: Post-yield Fracture Mechanics (2nd ed.), Latzko, D. G .H.(ed.), Elsevier Applied Science Publishers, New York, NY, 1984.
7. Sih, G. C., Am. Soc. Test. Mater. Proc. 605, 3-15 (1976).
8. Sih G. C., Introductory chapters in: Mechanics of Fracture, Vol. I to VII, Sih, G. C. (ed.), Martinus Nijhoff Publishers, The Netherlands, 1973-1982.
9. Hellen, T. K., Methods for computing contour integrals: Post-Yield Fracture Mechanics (2nd ed.), Latzko, D. G .H.(ed.), Elsevier Applied Science Publishers, New York, NY, 1984.
10. Park, J. M. and Thorpe, J. L., J. of Korea Tappi 28(4):17-30(1996).
11. Kohnke, P. C. (ed.) ANSYS Engineering Analysis System, Revision 4. 4. 5th ed., Houston, PA 15342, USA, Aug. 1, 1989.
12. Rance, H. F., Tappi, 39(2), 104-115 (1956).
13. ASTM E813-89, Standard Test Method for J_{IC}. A measure of fracture toughness, (1989).

*Recommended textbook : David Broek, Elementary Engineering Fracture Mechanics, 4th ed., Kluwer Academic Publishers, Boston, USA, pp.516, 1986.